

LA-UR- 96-4490

Approved for public release;
distrb.::tion is unlimited.

Title:

Nuclear Fuels Technologies
Fiscal Year 1996 Research and
Development
Test Results

Author(s):

C. A. Beard, H. T. Blair, J. J. Buksa,
D. P. Butt, K. Chidester, S. L. Eaton,
T. J. Farish, R. J. Hanrahan, K. B.
Ramsey

RECEIVED
FFR 14 1997
OSTI

Submitted to:

DOE Office of Fissile Materials
Disposition

Purpose: Programmatic Documentation

DISCLAIMER

This report was prepared as an account of work sponsored by an agency of the United States Government. Neither the United States Government nor any agency thereof, nor any of their employees, makes any warranty, express or implied, or assumes any legal liability or responsibility for the accuracy, completeness, or usefulness of any information, apparatus, product, or process disclosed, or represents that its use would not infringe privately owned rights. Reference herein to any specific commercial product, process, or service by trade name, trademark, manufacturer, or otherwise does not necessarily constitute or imply its endorsement, recommendation, or favoring by the United States Government or any agency thereof. The views and opinions of authors expressed herein do not necessarily state or reflect those of the United States Government or any agency thereof.

MASTER

Los Alamos
NATIONAL LABORATORY

Los Alamos National Laboratory, an affirmative action/equal opportunity employer, is operated by the University of California for the U.S. Department of Energy under contract W-7405-ENG-36. By acceptance of this article, the publisher recognizes that the U.S. Government retains a nonexclusive, royalty-free license to publish or reproduce the published form of this contribution, or to allow others to do so, for U.S. Government purposes. Los Alamos National Laboratory requests that the publisher identify this article as work performed under the auspices of the U.S. Department of Energy. The Los Alamos National Laboratory strongly supports academic freedom and a researcher's right to publish, as an institution, however, the Laboratory does not endorse the viewpoint of a publication or guarantee its technical correctness.

DISTRIBUTION OF THIS DOCUMENT IS UNLIMITED

LA-UR-96-4490

**Nuclear Fuels Technologies
Fiscal Year 1996 Research and Development Test Results**

**C. A. Beard, H. T. Blair, J. J. Buksa, D. P. Butt, K. Chidester,
S. L. Eaton, T. J. Farish, R. J. Hanrahan, K. B. Ramsey**

Los Alamos National Laboratory

November 8, 1996

DISCLAIMER

**Portions of this document may be illegible
in electronic image products. Images are
produced from the best available original
document.**

Table of Contents

TABLE OF CONTENTS.....	I
LIST OF FIGURES	I
LIST OF TABLES.....	II
1.0 INTRODUCTION.....	1
2. GALLIUM EVOLUTION TEST RESULTS.....	1
2.1. SURROGATE STUDIES	1
2.1.1. <i>Ga₂O₃ and CeO₂ Characterization</i>	1
2.1.2. <i>CeO₂-Ga₂O₃ Characterization</i>	2
2.1.3. <i>Phase Diagram Study</i>	3
2.1.4. <i>Thermodynamics and Kinetics of Gallium Oxide Vaporization</i>	3
2.2.0 PUO ₂ STUDIES	11
2.2.1. PUO ₂ THERMAL TREATMENT STUDY.....	11
2.2.2. EFFECT OF THERMAL TREATMENT ON FABRICATION STUDY.....	12
2.2.3. PIT CONVERSION DATA ASSESSMENT STUDY	13
2.2.4. PIT CONVERSION EXPERIMENTS	13
3.0 MOX FUEL FABRICATION TEST RESULTS.....	14
3.1. FEED CHARACTERIZATION STUDIES.....	14
3.1.1. <i>UO₂ Feed Characterization Study</i>	14
3.1.2. <i>PuO₂ Feed Characterization Study</i>	14
3.2. MOX FABRICATION STUDIES	14
3.2.1. <i>UO₂ Effect Study</i>	14
3.2.2. <i>Reference Fabrication Study</i>	17
3.2.3. <i>Pore Former Study</i>	17
3.3. PUO ₂ CONDITIONING STUDIES.....	17
3.2.1. <i>Mechanical Conditioning Study</i>	17

List of Figures

FIGURE 2.1.1-1. NON-ISOTHERMAL THERMOGRAVIMETRIC ANALYSIS OF GA ₂ O ₃ AND CeO ₂ EXPOSED TO AR-6% H ₂	2
FIGURE 2.1.4-1. CALCULATED EQUILIBRIUM PARTIAL PRESSURES ABOVE AGA ₂ O ₃ = 0.01 IN REDUCING ATMOSPHERES AND VACUUM.....	6
FIGURE 2.1.4-2. CALCULATED BINARY GASEOUS INTERDIFFUSION COEFFICIENT FOR GA ₂ O IN 1 ATM OF AR-6% H ₂ AT 1 ATM.....	7
FIGURE 2.1.4-3. CALCULATED KINEMATIC GAS VISCOSITY FOR AR-6% H ₂ AT 1 ATM.	8
FIGURE 2.1.4-4. CALCULATED SHERWOOD NUMBER FOR A 100 µM PARTICLE, IN A 500 CM/S FLOW OF AR-6% H ₂ AT 1 ATM.....	8
FIGURE 2.1.4-5. CALCULATED GALLIUM OXIDE FLUX FROM A 100 µM SPHERE OF PUO ₂ , ASSUMING A GA ₂ O ₃ ACTIVITY OF 0.01, IN AR-6% H ₂ AT 500 CM/S FLOW, 1 ATM.	10
FIGURE 2.1.4-6. TIME REQUIRED TO REMOVE GALLIUM FROM A 100 MM SPHERE OF PUO ₂ , ASSUMING A GA ₂ O ₃ ACTIVITY OF 0.01, IN AR-6% H ₂ AT 500 CM/S FLOW, 1 ATM.....	10

List of Tables

TABLE 2.1.2-1. ITEMS FOR THE MOX FUEL FABRICATION AND EVALUATION (COLD LAB).....	3
TABLE 2.1.2-2. AS-RECEIVED POWDERS USED IN FABRICATING SURROGATE FEED POWDERS.....	3
TABLE 2.1.2-3. RESULTS OF WEIGHT LOSS MEASUREMENTS FROM CeO_2 -2% Ga_2O_3 POWDER EXPOSED TO AR-6% H_2 AT 1000°C FOR 30 MIN.....	4
TABLE 2.1.4-1. SUMMARY OF CONSTANTS SHOWN IN EQUATION 1.....	4
TABLE 2.2.1-1 PLUTONIUM DIOXIDE POWDER CHARACTERISTICS FOLLOWING HEAT TREATMENT	11
TABLE 2.2.1-2 PLUTONIUM DIOXIDE POWDER CHARACTERISTICS FOLLOWING ADDITIONAL HEAT TREATMENT TESTS	11
TABLE 2.2.1-3 PARALLEL PLUTONIUM DIOXIDE POWDER CHARACTERISTICS FOLLOWING HEAT TREATMENT	12
TABLE 2.2.1-4 SIEVE ANALYSIS BEFORE AND AFTER GALLIUM REMOVAL TREATMENT	12
TABLE 2.2.2-1 EFFECT OF THERMAL TREATMENT ON MOX PELLET DENSITY	13
TABLE 2.2.3-1 PLUTONIUM DIOXIDE POWDER CHARACTERISTICS FOLLOWING HYDRIDE-OXIDATION ..	13
TABLE 3.1.1-1 ANALYSIS OF UO_2 SAMPLES FROM HANFORD AND AECL.....	15
TABLE 3.1.2-1 ANALYSIS OF PuO_2 FEED SOURCES.....	16
TABLE 3.2.2-1 ANALYSIS OF MOX PELLETS WITH AECL UO_2	17
TABLE 3.2.2-2 ANALYSIS OF MOX PELLETS WITH HANFORD UO_2	17

1.0 Introduction

During fiscal year 1996, the Department of Energy's Office of Fissile Materials Disposition (OFMD) funded Los Alamos National Laboratory (LANL) to investigate issues associated with the fabrication of plutonium from dismantled weapons into mixed-oxide (MOX) nuclear fuel for disposition in nuclear power reactors. These issues can be divided into two main categories: issues associated with the fact that the plutonium from dismantled weapons contains gallium, and issues associated with the unique characteristics of the PuO_2 produced by the dry conversion process that OFMD is proposing to convert the weapons material. Initial descriptions of the experimental work performed in fiscal year 1996 to address these issues can be found in *Nuclear Fuels Technologies Fiscal Year 1996 Research and Development Test Matrices*¹. However, in some instances the change in programmatic emphasis towards the Paralex program either altered the manner in which some of these experiments were performed (i.e., the work was done as part of the Paralex fabrication development and not as individual separate-effects tests as originally envisioned) or delayed the experiments into Fiscal Year 1997. This report reviews the experiments that were conducted and presents the results.

2. Gallium Evolution Test Results

2.1. *Surrogate Studies*

2.1.1. Ga_2O_3 and CeO_2 Characterization

Experiments conducted at LANL and Lawrence Livermore National Laboratory (LLNL) have shown that PuO_2 produced from weapons via the hydride-oxidation process still contains gallium, which after conversion exists in the form of its fully oxidized state, Ga_2O_3 . Initial thermogravimetric analysis (TGA) studies have been performed to characterize the kinetics of vaporization of Ga_2O_3 powder and pellets in Ar-6% H_2 (this reducing atmosphere is being used in the PuO_2 thermal treatment process, the fuel pellet sintering process, and is typical of the atmospheres used in commercial MOX pellet sintering furnaces). For comparison we have also investigated the kinetics of vaporization of CeO_2 , which is a surrogate material for PuO_2 . As shown in the non-isothermal TGA traces in Fig. 2.1.1-1, the vaporization rate for Ga_2O_3 becomes quite rapid at temperatures above about 1000°C. Difficulties were anticipated with these experiments because Ga will readily alloy with many metals, including Pt (the material used to suspend the samples in the furnace). As shown in Fig. 2.1.1-1, alloying between Pt and Ga leads to mechanical failure of the Pt near 1200°C.

The rapid vaporization of gallium oxide can have either negative or positive consequences. In particular, gallium loss can negatively affect the lifetime of components required for fuel fabrication or those in a nuclear reactor due to alloying. However, because it volatilizes, it may be possible to thermally separate gallium from PuO_2 relatively easily. It is critical to assess the thermodynamics and kinetics of the processes of vaporization of Ga_2O_3 - PuO_2 systems. It is also important to assess both the rate of loss of Ga and the loss of Pu. It is probable that Pu loss will be significant in a reducing atmosphere. Understanding the thermodynamics and kinetics will allow the minimization of Pu loss and maximization of Ga loss through the use of optimal processing conditions and vapor separation techniques.

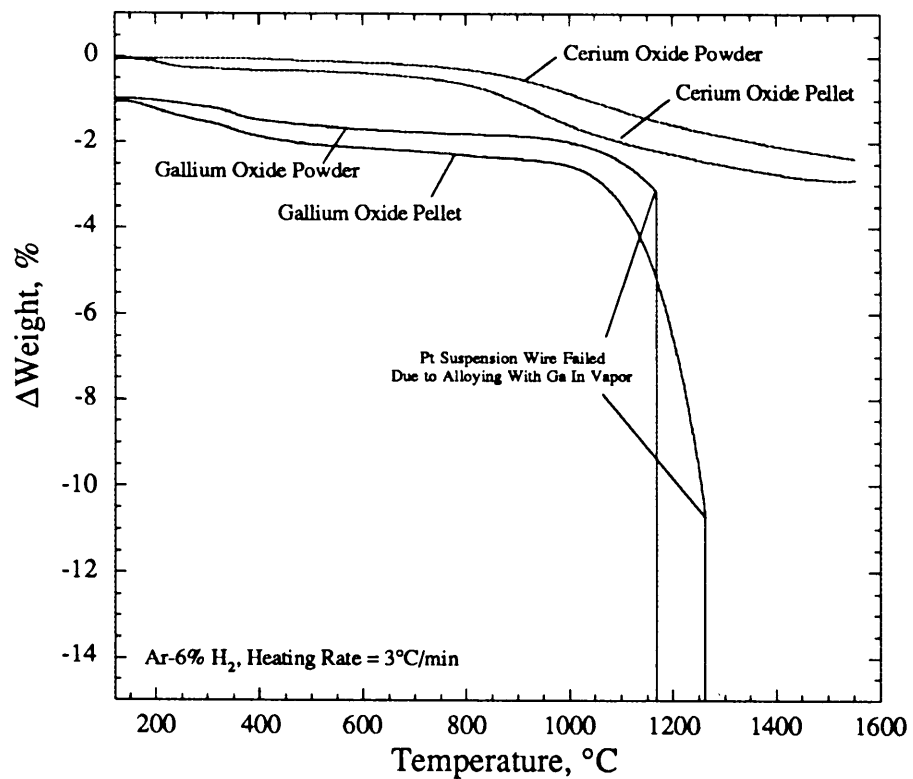


Figure 2.1.1-1. Non-isothermal Thermogravimetric Analysis of Ga_2O_3 and CeO_2 exposed to Ar-6% H_2 .

2.1.2. $\text{CeO}_2\text{-Ga}_2\text{O}_3$ Characterization

To determine the behavior of the gallium volatilization in a mixed-oxide media, CeO_2 -2wt% Ga_2O_3 pellets were fabricated with 95% theoretical density. Table 2.1.2-1 shows a list of the fabrication equipment in the cold (no plutonium) lab. CeO_2 -2 wt% Ga_2O_3 pellets were prepared using commercial powders (Table 2.1.2-2) and fabrication techniques similar to those used in preparing actual fuel. After preparation, the pellets were crushed to -325 mesh and the resulting powder exposed to Ar-6 % H_2 at 1000°C . The oxygen partial pressure was monitored during vaporization experiments, and was kept below 10^{-12} atm. To evaluate the effect of specimen size, the 0.3 and 0.9 gram samples were exposed to a slow flowing gas. Table 2.1.2-3 summarizes the experiments and illustrates the scatter in data. Two samples were analyzed, one weighing 0.3 g and a larger sample of 0.9 g. Assuming the entire weight loss of the sample was due to gallium volatilization, the 0.3 g sample lost on average 29.3% of its initial gallium content, while the 0.9 g sample only lost on average 10.7% of its gallium. The observation of variations in gallium loss with sample size indicates that the volatilization is at least partially rate limited by gas transport. These studies are continuing with the objective of collecting sufficient

Table 2.1.2-1. Items for the MOX fuel fabrication and evaluation (cold lab).

Process	Item	Model/Description
Weighing	Balance	Denver Instrument Co., A-160
Milling	Spex mill	SPEX mixer 8000
Pressing	Press	Carver model-6, range : 0-24000 lb.
Sieving	Screen	Dual MFG. Co. 40, 60, 80, 100 mesh
Sintering	Furnace	DelTec Inc. < 1750 °C
Vaporization	Furnace	Thermolyne 59300
Oxygen Measurement	O ₂ Monitor	Thermox CG1000 : Oxygen Analyzer

Table 2.1.2-2. As-received powders used in fabricating surrogate feed powders.

Powder	Supplier	Description
Gallium (III) oxide Ga ₂ O ₃	Johnson Mathey	99.999 % -325 mesh
Cerium (IV) oxide CeO ₂	Johnson Mathey	99.99 % 5 micron

data to model the Ga loss kinetics and comparing these data to the loss from PuO₂-based feed.

2.1.3. Phase Diagram Study

Although much of the information given in Section 2.1.4 forms the basis for generation of relevant phase diagrams, no specific phase diagrams were generated in FY96 (Note that in the FY96 test matrices, this task was designated to be performed only if funding permits). The phase diagram study will be carried out in FY97 in support of the integrated test program.

2.1.4. Thermodynamics and Kinetics of Gallium Oxide Vaporization

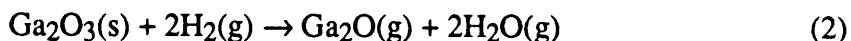
Thermodynamic data were collected and free energies of formation were fit, using stepwise multiple linear regression, to the equation:

Table 2.1.2-3. Results of weight loss measurements from CeO₂-2% Ga₂O₃ powder exposed to Ar-6% H₂ at 1000°C for 30 min.

Specimen Size	Total Weight Change in Specimen (wt-%)
0.3 g	0.4620
	0.6193
	0.9908
	0.5307
	0.3307
0.9 g	0.2332
	0.1869
	0.1992
	0.2105
	0.2420

$$\Delta G_f = a + bT + Tc^{-1} + dT^2 + eT^3 + fT\ln T \quad (1)$$

where *a-f* are constants, and *T* is temperature in Kelvin. Table 2.1.4-1 shows some of the data relevant to this brief summary of results. These data were used to calculate temperature dependent expressions for the vaporization behavior of gallium oxide from doped PuO₂. The atmospheres of interest are Ar-H₂ and CO/CO₂. Thus, temperature dependent expressions were determined from the mass action equations:



and

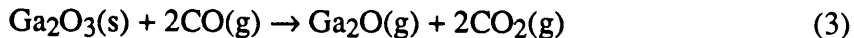


Table 2.1.4-1. Summary of constants shown in equation 1.

Compound	<i>a</i>	<i>b</i>	<i>c</i>	<i>d</i>	<i>e</i>	<i>f</i>
Ga ₂ O ₃ (s)	-1123572.	574.0020	2267569.	5.3080E-03	-6.8814E-07	-31.7864
Ga ₂ O(g)	-117031.	-55.3176	1295110.	8.3901E-03	-8.9622E-07	0
H ₂ O(g)	-236296.	-65.1431	-169071.	-6.2395E-03	4.2670E-07	16.6059
CO ₂ (g)	-391347.	-26.6122	-191047.	-4.0186E-04	0	3.2924
CO(g)	-104977.	-123.5504	-642559.	2.4364E-03	-2.8001E-07	3.8731

Using the data shown in the Table 2.1.4-1, the following equations were derived from which $\text{Ga}_2\text{O(g)}$ partial pressures can be calculated:

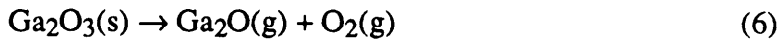
$$p_{\text{Ga}_2\text{O}} = \frac{a_{\text{Ga}_2\text{O}_3} p_{\text{H}_2}}{p_{\text{H}_2\text{O}}} \exp \left[91.3647 + 1.1203 \cdot 10^{-3}T - 7.761944 \cdot 10^{-8}T^2 - \frac{64223}{T} + \frac{157638}{T^2} - 7.8179 \ln T \right] \quad (4)$$

and

$$p_{\text{Ga}_2\text{O}} = \frac{a_{\text{Ga}_2\text{O}_3} p_{\text{CO}}}{p_{\text{CO}_2}} \exp \left[52.3747 + 3.1205 \cdot 10^{-4}T - 4.2332 \cdot 10^{-8}T^2 - \frac{52177.2}{T} + \frac{8351.7}{T^2} - 3.68355 \ln T \right] \quad (5)$$

Where a and p represent activity and equilibrium partial pressure, respectively.

In addition, the vaporization of $\text{Ga}_2\text{O(g)}$ may be assessed using the mass action equation:



where the partial pressure of $\text{Ga}_2\text{O(g)}$ may be calculated using the equation:

$$p_{\text{Ga}_2\text{O}} = \frac{a_{\text{Ga}_2\text{O}_3}}{p_{\text{O}_2}} \exp \left[75.69396 - 3.7071 \cdot 10^{-4}T + 2.50277 \cdot 10^{-8}T^2 - \frac{121066}{T} + \frac{117327}{T^2} - 3.82324 \ln T \right] \quad (7)$$

Equations (6) and (7) may be substituted for equations (2) through (5) by considering how the partial pressure of oxygen is controlled by either the $\text{H}_2/\text{H}_2\text{O}$ or CO/CO_2 ratios according to buffer reactions $\text{H}_2(\text{g}) + 1/2\text{O}_2(\text{g}) \rightarrow \text{H}_2\text{O}(\text{g})$, or $\text{CO}(\text{g}) + 1/2\text{O}_2(\text{g}) \rightarrow \text{CO}_2(\text{g})$.

The equations described above can be used to calculate the equilibrium partial pressures of Ga_2O above various $\text{PuO}_2\text{-Ga}_2\text{O}_3$ solid solutions (i.e., assuming various Ga_2O_3 activities) in inert atmospheres or H_2 - or CO -bearing gases. Fig. 2.1.4-1, shows how the vaporization behavior varies with environment at a Ga_2O_3 activity of 0.01, which is near the activity expected for a typical $\text{PuO}_2\text{-Ga}_2\text{O}_3$ feed stock. It is apparent from this figure that the vaporization rate in the reducing gases H_2 and CO is significantly higher than that in vacuum.

The thermodynamic data described above can be used to calculate the maximum rate of loss of gallium during processing of MOX fuel and powders. For example, using boundary layer theory and principals of gas kinetics, the maximum Ga loss rates from PuO_2 with $a_{\text{Ga}_2\text{O}_3} = 0.01$ have been calculated. In cases where the kinetics are rate limited by gaseous diffusion (which appears to be the case with MOX fuel and powder in certain environments) the calculated rates give very good estimates of the true loss rates as long as the activity of the species of interest (e.g. Ga_2O_3) is known. The flux of material, J , from a surface may be described using the equation:^{1,2}

$$J = \frac{DS_h}{dRT} p_i \quad (8)$$

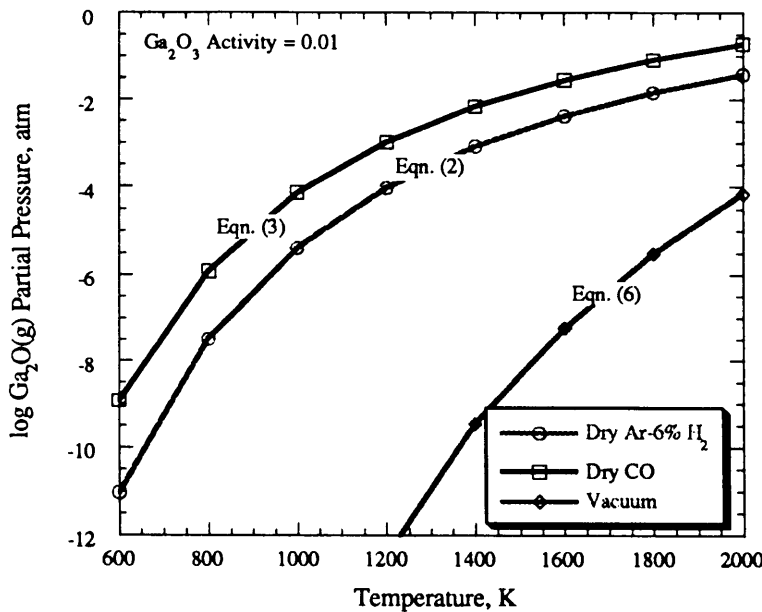


Figure 2.1.4-1. Calculated equilibrium partial pressures above $a_{Ga_2O_3} = 0.01$ in reducing atmospheres and vacuum.

where D is the binary interdiffusion coefficient, Sh is the Sherwood number, d is a characteristic dimension of the material, R is the universal gas constant, T is temperature, and p_i is the equilibrium partial pressure of the species of interest. For the sake of discussion, let us take a relatively simple case by assuming that we have a 100 μm , spherical particle. For a sphere, d is equal to the sphere diameter and the Sherwood coefficient may be defined as

$$Sh = 2.0 + 0.60 Re^{1/2} Sc^{1/3} \quad (9)$$

where Re is the Reynolds number and Sc is the Schmidt number. The Reynolds number is simply the dimensionless ratio of the inertial forces to viscous forces and may be defined as

$$Re = \nu d / \nu \quad (10)$$

where ν is the bulk gas stream velocity, d is (in this case) the sphere diameter, and ν is the kinematic gas viscosity. And the Schmidt number is simply the dimensionless ratio of the kinematic viscosity and the diffusion coefficient

$$Sc = \nu / D \quad (11)$$

All the parameters described in equations 8-11 may be calculated from first principals. We begin with the binary gaseous interdiffusion coefficient. If we assume we

have an Ar-6% H₂ gas mixture, the binary interdiffusion coefficient may be calculated using the equation:

$$D_{ij} = \frac{8\sqrt{\frac{2kT}{\pi}} \sqrt{\frac{1}{m_i} + \frac{1}{m_j}}}{3\pi(n_i + n_j)(r_i + r_j)^2} \quad (12)$$

where k is Boltzmann's constant, m is molecular mass, n is density of gas molecules per cubic meter, and r is the molecular diameter. Fig. 2.1.4-2 shows the calculated gaseous interdiffusion coefficient as a function of temperature for Ga₂O in Ar-6% H₂ at 1 atm.

Although the kinematic viscosities may also be calculated from Maxwellian principals, the viscosities for Ar and H₂ are well known.³ Thus, we used tabulated values of the individual dynamic viscosities, converted them to kinematic viscosities, and then calculated the viscosity of the two-component gas mixture using techniques described by Wilke⁴ and which have been demonstrated experimentally by Butt *et al.*⁵ Fig. 2.1.4-3 shows the kinematic viscosity of Ar-6% H₂ as a function of temperature at 1 atm.

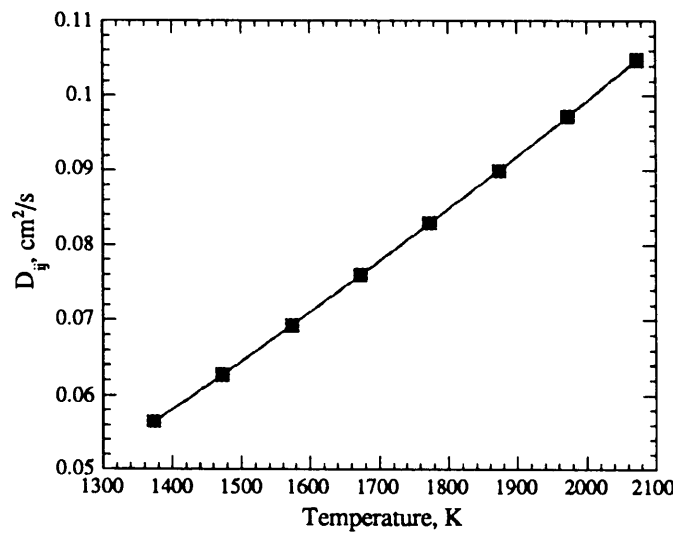


Figure 2.1.4-2. Calculated binary gaseous interdiffusion coefficient for Ga₂O in 1 atm of Ar-6% H₂ at 1 atm.

With knowledge of D_{ij} and ν , the Reynolds and Schmidt numbers can be easily calculated using equations 10 and 11. For the purpose of discussion, assume simplistically that we have 100 μm diameter particles are exposed to Ar-6% H₂ at a gas velocity of 500 cm/sec. Under this assumption, the Sherwood number can then be calculated using equation 9 as illustrated in Fig. 2.1.4-4.

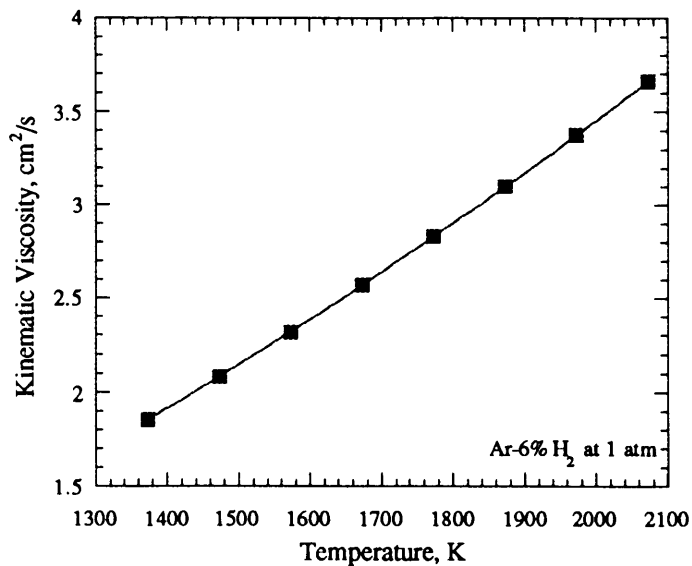


Figure 2.1.4-3. Calculated kinematic gas viscosity for Ar-6% H₂ at 1 atm.

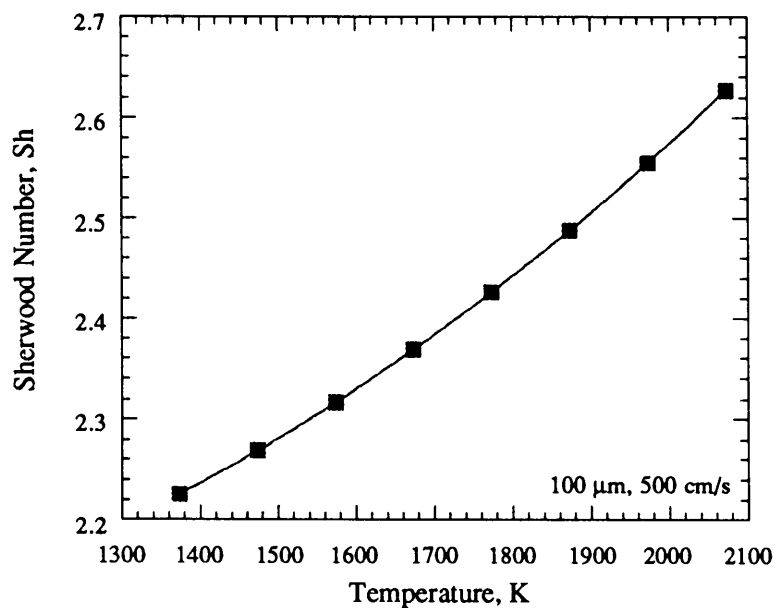


Figure 2.1.4-4. Calculated Sherwood number for a 100 μm particle, in a 500 cm/s flow of Ar-6% H₂ at 1 atm.

For convenience, D_{ij} , v , Re , Sc , and Sh under these conditions are described using the following polynomial equations:

$$D_{ij} = -9.7 \cdot 10^{-3} + 3.439 \cdot 10^{-5}T + 1.005 \cdot 10^{-8}T^2 \text{ cm}^2/\text{s} \quad (13)$$

$$v = -0.341 + 9.434 \cdot 10^{-4}T - 4.768 \cdot 10^{-7}T^2 \text{ cm}^2/\text{s} \quad (14)$$

$$Re = 9.432 - 6.928 \cdot 10^{-3}T + 1.467 \cdot 10^{-6}T^2 \quad (15)$$

$$Sc = 2.077 - 3.557 \cdot 10^{-3}T + 1.856 \cdot 10^{-6}T^2 \quad (16)$$

$$Sh = 2.127 - 2.593 \cdot 10^{-4}T + 2.414 \cdot 10^{-7}T^2 \quad (17)$$

Thus, through equation 8, the corrosion flux can now be calculated using equations 4, 13, and 17. Fig. 2.1.4-5 shows the calculated Ga_2O flux as a function of temperature using the assumptions stated above and assuming the $a_{\text{Ga}_2\text{O}_3}$ is 0.01. As is apparent from Fig. 2.1.4-5, the calculated (or projected) rates of vaporization are quite rapid. It must be re-emphasized that these calculated rates are maximum rates. Using these maximum rates, the time to remove gallium from a 100 μm sphere is shown in Fig. 2.1.4-6. In reality the rates will be reduced by a number of parameters, such as backing gas pressures in powder compacts, changes in the Ga_2O_3 activity as vaporization proceeds, changes in metal/oxygen stoichiometry, and (depending on the rate limiting mechanism) reductions by a chemical reaction (e.g., adsorption or desorption of a molecule). As implied here, the model described above assumes a constant Ga_2O_3 activity. In order to make full use of the model, we require information on the diffusivities of gallium oxides in PuO_2 as well as how the overall stoichiometry affects the diffusion and activity. As described by Wallace and Butt,⁶ although it is a very difficult and rigorous task, in theory it is possible to combine solid state and gaseous diffusion equations to describe the gas solid reactions under conditions that are rate limited by gas transport where the partial pressures vary continuously due to solid state diffusion and changes in stoichiometry. However, in the case of this particular system, we are lacking much of the necessary kinetic data.

The modeling and results described above can ultimately be used in the design of a large-scale Ga removal process, including tradeoffs between alternative processing equipment.

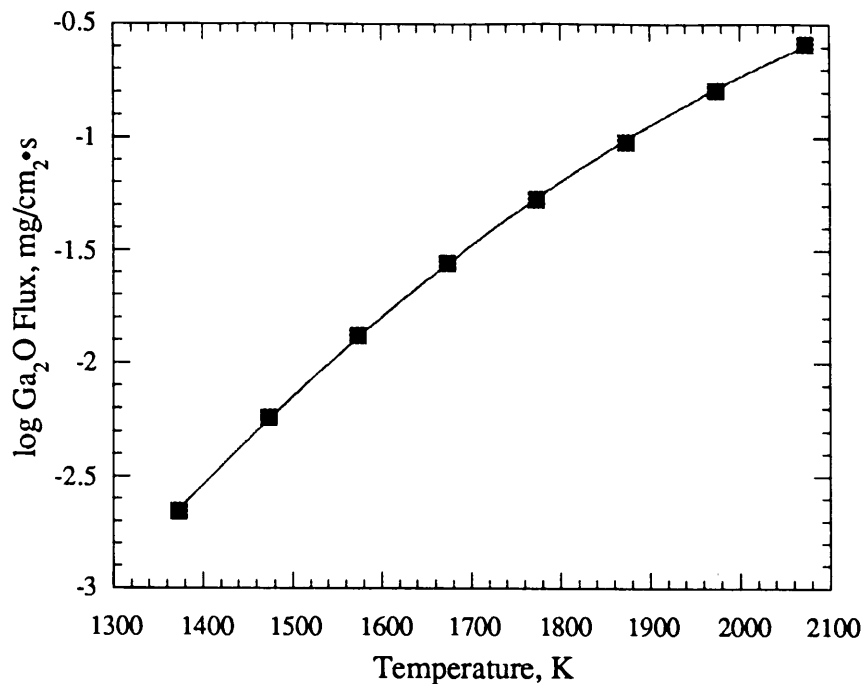


Figure 2.1.4-5. Calculated gallium oxide flux from a 100 μm sphere of PuO_2 , assuming a Ga_2O_3 activity of 0.01, in Ar-6% H_2 at 500 cm/s flow, 1 atm.

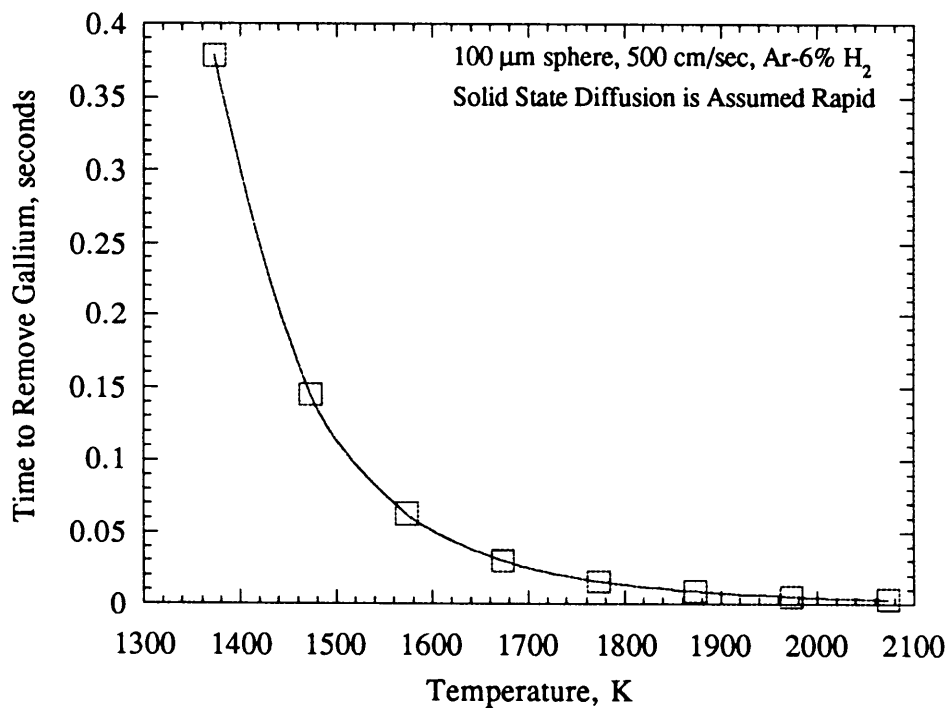


Figure 2.1.4-6. Time required to remove gallium from a 100 μm sphere of PuO_2 , assuming a Ga_2O_3 activity of 0.01, in Ar-6% H_2 at 500 cm/s flow, 1 atm.

2.2.0 *PuO₂* Studies

2.2.1. *PuO₂* Thermal Treatment Study

The *PuO₂* thermal treatment study examines the thermal volatilization of *Ga₂O₃* from actual *PuO₂* (as opposed to surrogates). It is used to establish basic data as well as benchmark the surrogate studies.

Separate samples of the *PuO₂* powder produced at LANL in FY 1995 (LANL-FY95 in Table 2.2.3-1) were heated in flowing Ar-6%H₂ at 400 °C and 1000 °C, respectively, for two hours to determine the effects on gallium content and particle properties. These results are given in Table 2.2.1-1. As evident from these results, heat treating the powder at 400 °C (LANL-3) had little effect on the gallium content, particle size, and surface area. However, heat treating at 1000 °C (LANL-4) did reduce the gallium content and surface area considerably. The high temperature treatment may also have reduced the oxide to a hypostoichiometric condition as suggested by the negative loss-on-ignition results. Consequently, gallium can be removed from the *PuO₂* by thermal treatment, but the physical properties of the powder that will affect its performance in the fabrication of MOX fuel may be altered.

Table 2.2.1-1 Plutonium Dioxide Powder Characteristics Following Heat Treatment

Powder Identification	Description	Gallium Content (ppm)	Mean Particle Size (μ)	Surface Area (m ² /g)	Loss On Ignition (wt%)
LANL-1	As received	5030	14.7	5.52	NA
LANL-3	2 hours @ 400 °C	5017	12.3	5.1	0.04
LANL-4	2 hours @ 1000 °C	365	13.6	0.7	-0.19

Additional thermal treatment experiments were conducted using some of the LANL-FY95 plutonium dioxide. The material was heated for 2 or 4 hours in flowing Ar-6%H₂ at temperatures ranging from 900 C to 1100 C, and the gallium content measured. Because the negative loss-on-ignition result in the earlier test indicated the possibility the powder was hypostoichiometric, the oxygen-to-metal ratio was also measured. The results of the analyses are shown in Table 2.2.1-2.

Table 2.2.1-2 Plutonium Dioxide Powder Characteristics Following Additional Heat Treatment Tests

Treatment	Gallium Content after Treatment (ppm)	O/M
2 Hours at 900 C	918	1.995
4 Hours at 1000 C	312	2.006
2 Hours at 1100 C	125	1.994

Based on the above results, a preliminary gallium removal treatment was developed. This treatment involves treating the *PuO₂* for 2 hours at 1100 C in Ar-6%H₂ to remove the gallium, followed by heating for 2 hours at 800 C in air to re-establish stoichiometry. This treatment was used on 500 g batches of the Parallex *PuO₂*. The results

for the treatment of the Paralex PuO₂ are shown in Table 2.2.1-3. The gallium in this material was only reduced to 243 ppm due to the larger batch size and larger initial gallium content. However, this is still sufficient to reduce the gallium to less than 10 ppm in the final MOX fuel. It should also be noted that no significant reduction in surface area was observed, which contradicts earlier results (see Table 2.2.1-1). This discrepancy will have to be resolved in future work. A sieve analysis was conducted before and after the thermal treatment to determine the effects on particle size distribution. The results of the analyses are shown in Table 2.2.1-4. However, for the after-treatment results reported, an error was made in the furnace settings for the oxidizing step which resulted in the powder being treated at 1000 C for 48 hours (instead of 2 hours at 800 C). Even under these more extreme conditions, no significant changes in the particle size distribution was observed.

Following the treatment of approximately 2 kg of PuO₂, deposits were visually observed on the heat shields of the furnace. These deposits were analyzed and found to be mostly gallium (67%) and uranium (23%). The presence of uranium is due to the use of this furnace in the fabrication of uranium-nitride for an earlier program.

Table 2.2.1-3 Paralex Plutonium Dioxide Powder Characteristics Following Heat Treatment

Treatment Variables	Gallium Content (ppm)	Mean Particle Size (μ)	Surface Area (m ² /g)	Oxygen-to-Metal Ratio
As received	8575	17.4	6.85	2.281
1100 C for 2 hr in Ar-6%H ₂ , then 800 C for 2 hr in air	243	17.0	6.84	2.034

Table 2.2.1-4 Sieve Analysis Before and After Gallium Removal Treatment

Mesh Size	As received (Wt %)	After Treatment (Wt %)
+140	4.38	6.56
-140 to +170	5.58	2.41
-170 to +200	3.26	3.49
-200 to +230	2.42	2.86
-230 to +325	9.57	7.78
-325	74.78	76.90

2.2.2. Effect of Thermal Treatment on Fabrication Study

In order to investigate the effects of thermal treatment on MOX pellet fabrication, two batches of MOX fuel pellets were fabricated using the LANL-FY95 PuO₂ feed and Hanford UO₂ powder. One batch of 10 pellets used the baseline fabrication process, while a second batch of 15 pellets was fabricated using the same feed sources and fabrication process, but with the addition of a thermal treatment step to remove Gallium from the PuO₂ prior to pellet fabrication (the PuO₂ was heated for 2 hours in Ar-6%H₂ at 1100 C, but the treatment did not include the oxidation step). Both batches were sintered for 4 hours at 1725 C. As shown in Table 2.2.2-1, pellets fabricated with untreated PuO₂ achieved 93.24% of theoretical density, while pellets fabricated with thermally treated PuO₂ achieved 93.49% of theoretical density. However, it should be noted that the UO₂-PuO₂ blends for both these pellet types were vibratory milled in order to increase pellet density. This vibratory milling may have eliminated any effects of the PuO₂ treatment. Details of the composition of the PuO₂ and UO₂ powders used in this study are shown in Table 3.1.2-1

and Table 3.1.1-1 respectively. Little effect was seen in the %theoretical density achieved between the treated and untreated PuO_2 powders. Although an analysis of the microstructure of these pellets was not made due to a shift of programmatic emphasis to the Paralex project, such analyses were made of subsequent batches of pellets which showed no adverse effects of the thermal treatment on microstructure (all Paralex fuel was fabricated using thermally treated PuO_2 and no adverse effects on grain size or homogeneity were observed.).

Table 2.2.2-1 Effect of Thermal Treatment on MOX Pellet Density

PuO_2 Powder Treatment	Density (% Theoretical Density)
Thermally Treated PuO_2	93.49
Untreated PuO_2	93.24

2.2.3. Pit Conversion Data Assessment Study

The purpose of this study is to develop a database of pit conversion data related to Ga loss and PuO_2 physical characteristics as a function of conversion variables (such as time, temperature, atmosphere, weapon type, etc.).

In FY95, plutonium dioxide produced from a dismantled weapon by the hydride-oxidation process at LANL was obtained. Additionally, two different plutonium oxide powders produced at LLNL were obtained from a single weapon using the HYDOX process at either 125C or 400 C as the hydride temperature. The powder converted at 400 C was also ground at LLNL with a mortar and pestle to pass through a 20-mesh sieve. In FY96, additional PuO_2 produced at LANL by hydride-dehydride (to a puck) followed by hydride-oxidation of the resulting metal was obtained. Samples of each material were analyzed for gallium content, particle size, surface area and loss on ignition. The results of these analyses are given in Table 2.2.3-1. The results show that the gallium content of the oxide produced at LANL is the same as it was in the metal before the conversion to oxide (the first LANL PuO_2 was 0.5 wt% gallium, and the second batch had 0.8 wt% initial gallium content). However, the gallium content of the oxides from LLNL were reduced by the conversion process from the original 1 wt%.

Table 2.2.3-1 Plutonium Dioxide Powder Characteristics Following Hydride-Oxidation

Powder Identification	Description	Gallium Content (ppm)	Mean Particle Size (μ)	Surface Area (m^2/g)	Loss On Ignition (wt%)
LANL-FY95	hydride-oxidation	5030	14.7	5.5	0.29
LLNL-1	400 C and ground	6472 to 8365	16.5	0.8	-0.04
LLNL-2	125 C	2390	39.3	3.0	0.02
Paralex PuO_2	hydride-dehydride, hydride-oxidation	8575	17.5	6.8	0.15

2.2.4. Pit Conversion Experiments

This task was not performed during FY96. (Note that in the FY96 test matrices, this task was designated to be performed only if funding permitted). The behavior of Ga in the pit conversion process will be included as part of the FY97 plan in both nuclear fuels technologies as well as the ARIES demo.

3.0 MOX Fuel Fabrication Test Results

3.1. *Feed Characterization Studies*

3.1.1. **UO₂ Feed Characterization Study**

This study characterized two samples of UO₂ similar to that used in commercial power reactor fuel fabrication. One sample was obtained from Hanford, and the other from AECL. Both were analyzed at LANL to determine uranium content, mean particle size, surface area, uranium isotopics and elemental composition. The AECL sample was also analyzed at AECL prior to shipment to LANL. The results of these analyses are listed in Table 3.1.1-1. Multiple entries in the table indicate that more than one analysis was performed.

3.1.2. **PuO₂ Feed Characterization Study**

Two sources of PuO₂ were used in FY96 efforts. First, in FY95 PuO₂ was produced by hydride-oxidation of weapons components (LANL-FY95). In fiscal year 1996, 2.9 kg of PuO₂ were produced for the Paralex program at LANL. A plutonium metal puck was produced from surplus weapons components using a hydride-dehydride process, and then the puck was converted to PuO₂ using hydride-oxidation ("Paralex" PuO₂). Significant magnesium contamination of the "Paralex" PuO₂ resulted from the use of a magnesium crucible with the hydride-dehydride processing, which is not envisioned for use in the future production of oxide with direct hydride-oxidation of weapons components. Each PuO₂ source was analyzed to determine plutonium content, loss on ignition (LOI), mean particle size, surface area, plutonium isotopics and elemental composition, including gallium and oxygen content after various treatment processes. The results of these analyses are listed in Table 3.1.2-1.

3.2. *MOX Fabrication Studies*

3.2.1. **UO₂ Effect Study**

Pellets were fabricated with both Hanford and AECL UO₂. However, a single sintering run was not performed with pellets of both types because once the AECL UO₂ was available, all of the fabrication activities were focused on the Paralex program. However, no discernible differences were observed between the two UO₂ sources, and, as shown in section 3.1.1, their physical properties were very similar with the exception of surface area. Data on pellets fabricated with both the Hanford and AECL UO₂ are given in section 3.2.2.

Table 3.1.1-1 Analysis of UO₂ Samples from Hanford and AECL

Parameter	Hanford UO ₂ (LANL Analysis)	AECL UO ₂ (AECL Analysis)	AECL UO ₂ (LANL Analysis)
% Uranium	87.35	87.12	86.82
Mean Particle Size (μ)	3.3 2.7		3.3 3.0
Surface Area (m ² /g)	2.8232 2.3447 3.1846		5.4137 5.0155 5.5309
Uranium Isotopes (w/o):			
U-234	0.0012 0.0012		0.0014 0.0014
U-235	0.2240 0.2425	0.26	0.2689 0.2748
U-236	0.0025 0.0028		0.0015 0.0007
U-238	99.7723 99.7535		99.7283 99.7231
Elemental Analysis (ppm):			
Al		15	
B		< 0.1	
C	1300	140	
Ca		15	
Cd		< 0.2	
Cl	52.2, 50		
Cr		7	
Cu		2	
F	242.7, 245	50	
Fe		240	
Mg		2	
Mn		3	
Mo		1.4	
Ni		10	
S	23.8, 10		
Si		15	< 20

Table 3.1.2-1 Analysis of PuO₂ Feed Sources

Parameter	LANL-FY95	Parallex PuO ₂
Pu Content (%)	86.69	85.85 85.82 85.84
Loss on Ignition	0.29030 0.28597	0.2963 0.0135
Mean Particle Size (μ)	14.5 14.8 14.6	16.9 18.1
Surface Area (m ² /g)	5.2853 5.7349 5.5421	7.1645 6.3513 7.0168
Plutonium Isotopes (w/o):		
Pu-238	0.0221 0.0204	0.0123 0.0126
Pu-239	93.8127 93.8133	93.9528 93.9368
Pu-240	5.8823 5.8817	5.8439 5.8454
Pu-241	0.2468 0.2486	0.1396 0.1394
Pu-242	0.0362 0.0360	0.0514 0.0658
Elemental Analysis (ppm):		
Am	1520	1450, 1530, 1490
C	0.1330, 0.1058	0.13, 0.038, 0.068
Cl		34, 22, 18
F		15, <125, 11
Fe	310	
S		674, 121, <22
Mg		> 3000
Gallium Analysis:		
as received	5100 5043 5017	8504 8646
after treatment		239 244 250
O/Pu Analysis (as received):		2.281

3.2.2. Reference Fabrication Study

All of the pellets fabricated for the Paralex program were fabricated with the AECL UO₂ using a double-batching process. A 10% Pu in heavy elements master blend was made that was then down-blended to the desired 3.1% Pu in heavy metal. The pellets were sintered at 1725 C for 8 hours. Moisture was introduced into the sintering atmosphere to produce the required oxygen-to-metal ratio (O/M) of 1.995-2.015. The characteristics of these pellets are given in Table 3.2.2-1.

Table 3.2.2-1 Analysis of MOX Pellets with AECL UO₂

Parameter	MOX with AECL UO ₂	
Sintering Time (hr)		8
Sintering Temperature (°C)		1725
Theoretical Density (%)		95.96
O/M		2.005
Grain Size (μ)		11.1

Two batches of MOX pellets made with Hanford UO₂ were fabricated using different sintering times and temperatures. The pellets were than analyzed for % theoretical density. Results are shown in Table 3.2.2-2.

Table 3.2.2-2 Analysis of MOX Pellets with Hanford UO₂

Parameter	MOX with Hanford UO ₂	
Sintering Time (hr)	4	16
Sintering Temperature (°C)	1600	1700
Theoretical Density (%) Analysis 1	92.71	94.13
Analysis 2	92.94	93.86

3.2.3. Pore Former Study

While the pore former currently used by a commercial fuel vendor in MOX fuel fabrication was obtained, this study was not completed because of the shift of emphasis to the Paralex project (the pore former study is not applicable to CANDU fuel). It is expected that this study will be completed as part of the development activities for the LWR demonstration project in Fiscal Year 1997.

3.3. PuO₂ Conditioning Studies

3.2.1. Mechanical Conditioning Study

Following the thermal treatment of the Paralex PuO₂, a mechanical conditioning step was added. This conditioning step consisted of passing the PuO₂ powder three times through the vibratory mill prior to blending with UO₂. Using a scanning-electron microscope (SEM), the homogeneity of pellets produced with this PuO₂ was compared with that of pellets produced from PuO₂ that did not undergo a mechanical conditioning step. Initial data indicates that the mechanical conditioning resulted in an increase in homogeneity of the PuO₂ with no particles greater than 2μ being observed in the matrix, compared with maximum particle sizes of 10-20μ being observed for the non-mechanically

treated material. However, there was also a variation in sintering temperature (1725 C vs. 1600 C) and sintering time (8 hours vs. 4 hours) that could also account for part or all of this variation. Further work is necessary to determine the exact relationship between homogeneity and mechanical conditioning of the PuO₂. However, it should be noted that no results to date have indicated that mechanical conditioning of the PuO₂ is required in order to fabricate acceptable fuel pellets.